

Importance of a proper treatment of ice crystal sedimentation for cirrus clouds in large-scale models

Peter Spichtinger^{1*}, Klaus Gierens² and Ulrike Lohmann¹

(1) Institute for Atmospheric Science and Climate, ETH Zurich, 8092 Zurich, Switzerland

(2) Institut für Physik der Atmosphäre, Deutsches Zentrum für Luft- und Raumfahrt, Oberpfaffenhofen, Germany

1. Introduction

Nowadays large scale models of the atmosphere like weather forecast models and general circulation (climate) models usually have one prognostic variable to represent the ice phase in the upper troposphere, namely the cloud ice mixing ratio. However, microphysical and radiative properties of cirrus clouds depend sensitively on the size of the ice crystals; thus it is desirable to have also the number concentration of the crystals as a prognostic variable. While such double-moment schemes are almost state of the art in cloud resolving modeling, this is not the case in large scale models. However, the only examples of such double moment schemes are a special version of the ECHAM general circulation model (Lohmann 2002; Lohmann and Kärcher 2002) and a special version of the NCAR GCM (Ghan et al. 1997). The proper representation of clouds in large-scale models is still fraught with a multitude of difficulties. The first-order problem for a proper representation of cirrus clouds in large scale models is the combination of small- and large-scale dynamics that induces formation of these clouds (DelGenio 2002). However, also the processes within the cirrus clouds and the interactions of the cirrus and their supersaturated surroundings are important, because they control the optical properties and the lifetime of the clouds as will be discussed below. One particular point in this respect is the representation of ice crystal fall speeds. Ice crystals fall relative to the ambient air due to gravity. This gravitational set-

ting is an important structure building process in clouds, as big crystals fall faster than small crystals. Typically, in a cirrus cloud the top of the cloud (where the crystals are nucleated) contains small but numerous ice crystals, whereas the bottom of the cloud consists of a few large crystals. This structure implies that there are vertical gradients of optical properties in cirrus clouds, such that different cloud layers can have different cooling or warming effects (Khvorostyanov and Sassen 2002). Atmospheric models are generally very sensitive to the treatment of cloud ice, but because of the importance of sedimentation for the cloud structure the models are particularly sensitive to the numerical formulation of sedimentation. Jakob (2002) has demonstrated that, in the weather forecast model of the European Centre for Medium Range Weather Forecast (ECMWF), the global mean integral radiation flux divergence decreases from 110 W m^{-2} to 90 W m^{-2} for assumed fixed values of the crystal fall-speed of 0.1 and 2 m s^{-1} , respectively. The difference of 20 W m^{-2} , although resulting from extreme assumptions, is tremendous when compared with the 3.5 W m^{-2} radiative forcing due to the greenhouse effect for doubling CO_2 . Hence, the treatment of sedimentation in large scale models must be done with extreme care.

In the forthcoming models that have both crystal number density and ice mass concentration as prognostic values, one has the chance of an improved mapping of the real world cloud structure into the model world. This can be achieved by using different fall velocities for crystal number and crystal mass. This is not a novel strategy because it has been implemented in many cloud resolving models since 1978 when Srivastava (1978) used

*peter.spichtinger@env.ethz.ch

it probably for the first time in a model of warm clouds. However, to implement this concept in a GCM is something new. Here we review the strategy and formulate it as a derivation from a flux density concept, and we show as an illustration its effects on the cloud structure, radiative properties, and cloud lifetime using a single-column model with high vertical resolution.

2. Treatment of ice crystal sedimentation in a two-moment scheme

The flux density concept allows to formulate sedimentation in double-moment schemes in a coherent way once the analytical type of crystal mass distribution $f(m)$ is specified. This specification does not mean that $f(m)$ cannot vary with time; only the distribution type is fixed, its parameters vary with time according to the cloud evolution. The *a priori* specification of a certain kind of mass (or size) distribution is inevitable in a bulk scheme. For the mass distribution we assume the following normalisation:

$$\int_0^\infty f(m) dm =: \mu_0 = N,$$

that is, the moment of order zero, μ_0 , equals the number of ice crystals per unit volume. With this normalisation, the mean value of a quantity x with respect to $f(m)$, \bar{x} is given by

$$\bar{x} = N^{-1} \int_0^\infty x(m) f(m) dm$$

and the general moment is $\mu_k = \int m^k f(m) dm$, so that the mean mass is $\bar{m} = \mu_1/\mu_0$. The sedimentation is defined via the number and mass flux densities, respectively, namely:

$$\text{number flux density } f_n := N \cdot v_{t,n} \quad (1)$$

$$\text{mass flux density } f_m := \text{IWC} \cdot v_{t,m}. \quad (2)$$

Here, $\text{IWC} = N\bar{m}$ is the mass of ice per unit volume (usually termed ice water content), and $v_{t,n}, v_{t,m}$ are corresponding bulk terminal velocities for number and mass, respectively.

It is straightforward to define $v_{t,n}$ with use of $f(m)$:

$$Nv_{t,n} = N\bar{v}_t = \int_0^\infty v_t(m) f(m) dm,$$

hence $v_{t,n} \equiv \bar{v}_t$. For $v_{t,m}$ we have

$$\text{IWC } v_{t,m} = N\bar{m}\bar{v}_t,$$

so that $v_{t,m} = \bar{m}\bar{v}_t/\bar{m}$. Here, obviously, $v_{t,m} \neq v_{t,n}$, and we have two different sedimentation velocities in the model. Let us also assume that v_t depends on the crystal mass in the following way:

$$\left(\frac{v_t(m)}{V}\right) = \alpha \left(\frac{m}{M}\right)^\beta,$$

where V, M are unit velocities and masses, respectively, and α, β are certain parameters, that depend on the crystal habit. Such a relation between ice crystal mass and fallspeed can be traced back to the empirical relationships derived by Heymsfield (1972) and was applied already in the cirrus model of Starr and Cox (1985). But also the most recent papers on ice crystal terminal velocities (e.g. Heymsfield and Iaquinta 2000) suggest relations of this type.

When the parameters α, β are constants, the fallspeeds can directly be formulated via the general moments μ_k of the mass distribution, viz.

$$\left(\frac{v_{t,n}}{V}\right) = \frac{\alpha}{M^\beta} \frac{\mu_\beta}{\mu_0} \quad (3)$$

and

$$\left(\frac{v_{t,m}}{V}\right) = \frac{\alpha}{M^\beta} \frac{\mu_{\beta+1}}{\mu_1}. \quad (4)$$

These expressions are valid for any assumed mass distribution as long as the moments exist up to the order $\beta + 1$.

Since large particles fall faster than small ones, $v_{t,m} > v_{t,n}$ must be valid for any *a priori* choice of a mass distribution. This implies the following inequality between the moments:

$$\mu_{\beta+1}\mu_0 \geq \mu_\beta\mu_1. \quad (5)$$

This inequality is valid for all probability distributions that are defined only on the non-negative real axis. This assures that whatever mass distribution we specify in the initialisation of a model run, and whatever may evolve from it in the course of the simulation, the inequality $v_{t,m} > v_{t,n}$ is always obeyed.

3. Description of the reference simulations and microphysical results

For our study we implement a double-moment bulk ice microphysics scheme for cold temperature regions (i.e. $T < -38^\circ\text{C}$) into the 3D anelastic, non-hydrostatic model EuLag (see e.g. Smolarkiewicz and Margolin 1997). We use the microphysical variables water vapour mixing ratio, ice water mixing ratio, and ice crystal number density. The following microphysical processes are included for this study: deposition growth and evaporation of ice crystals (Koenig 1971; Gierens 1996), and sedimentation as described in section 2, including the possibility to use the same terminal velocity for ice water content and for ice crystal number densities, so that these two approaches and their impact on the simulated clouds can be compared. In contrast to other models all ice crystals start to fall relative to the ambient air once they are formed, i.e. there are no different classes for cloud ice and sedimenting ice. Crystal aggregation is not yet implemented in our microphysics code. Although aggregation could in principle modify quantitatively the results of our study, the basic findings would probably be unaffected, in particular because ice-ice aggregation at cold temperatures does not seem to be an important process outside of cumulonimbus anvils, hurricanes, or mesoscale convective systems (see e.g. Kajikawa and Heymsfield 1989). We carry out several numerical simulations to investigate the effect of equal vs. different terminal velocities for a model cloud. For this purpose we use the following setup:

We run EuLag as a single column model in the vertical range between 0 and 14 km with 50 m vertical resolution (i.e. 281 vertical levels). In this domain we initialize the vertical profiles for pressure, density, temperature and relative humidity according to the anelastic profiles by Clark and Farley (1984) as representing atmospheric conditions for an idealized atmosphere with constant stability; here we assume a Brunt-Vaisala frequency $N = 0.0094 \text{ s}^{-1}$, i.e. an almost constant temperature gradient $dT/dz \approx 0.0078 \text{ K/m}$. At $z_{TP} = 12 \text{ km}$ we prescribe the tropopause with a change in the temperature gradient: for $z > z_{TP}$ we again assume an almost

linear gradient of $dT/dz \approx 0.0016 \text{ K/m}$. The temperature profile is representative for midlatitude spring conditions. We choose the following relative humidity profile: In the range $10500 \leq z \leq 11500 \text{ m}$ a saturated cloud layer (i.e. $RHi(z) = 100\%$) of thickness $\Delta z = 1 \text{ km}$ is initialized. Down to the surface the relative humidity is constant and subsaturated ($RHi_1 = 60\%$). Above the cloud layer the relative humidity is also constant and subsaturated ($RHi_3 = 5\%$).

An idealized cirrus cloud is initialized in the saturated layer in the range $10500 \leq z \leq 11500 \text{ m}$. We prescribe ice crystal number density ($N_c = 100 \text{ L}^{-1}$) and ice water content (i.e. $\text{IWC} = 10 \text{ mg m}^{-3}$). As we use bulk microphysics, we have to prescribe a distribution type for the ice crystal mass. In our case, the ice crystal mass is log-normally distributed with constant geometric standard deviation σ_m and initial geometric mean mass

$$m_0 = \frac{\text{IWC}}{N_c \cdot \exp\left(\frac{1}{2}(\log(\sigma_m))^2\right)} \quad (6)$$

For our simulations we set $\sigma_m = 3.25$, the equivalent value for the size distribution using the mass-length-relation acc. to Heymsfield and Iaquinta (2000) ($m/M = a \cdot (l/L)^b$) is $\sigma_l = 1.71$. All crystals are assumed to be of column habit. The simulation time is $t = 4 \text{ h}$ with a timestep of $dt = 1 \text{ s}$. We run the model for two kinds of simulations: In the first type we use the same terminal velocity for ice water content and for ice crystal number density, namely $v_{t,n} = v_{t,m} = \overline{mv_t}/\overline{m}$. In the second kind we use different terminal velocities for ice water content and for ice crystal number density, namely $v_{t,n} \neq v_{t,m}$.

The two sedimentation schemes lead to completely different cloud structures in all simulations that we have run. Here we show in particular the mean crystal lengths for several time instances (every hour) as a function of altitude. Some important differences between the two simulations can be observed: When sedimentation is the same for ice mass and number concentrations, then the mean crystal mass (or mean crystal length) stays nearly constant during the 4 hr simulation time; the size distribution changes little with time and little with the vertical position in the cloud. The cloud seems to sink down almost as a solid body, which is unrealistic. The situation changes dramatically, when two different terminal velocities are used. This results in small crystals at the cloud

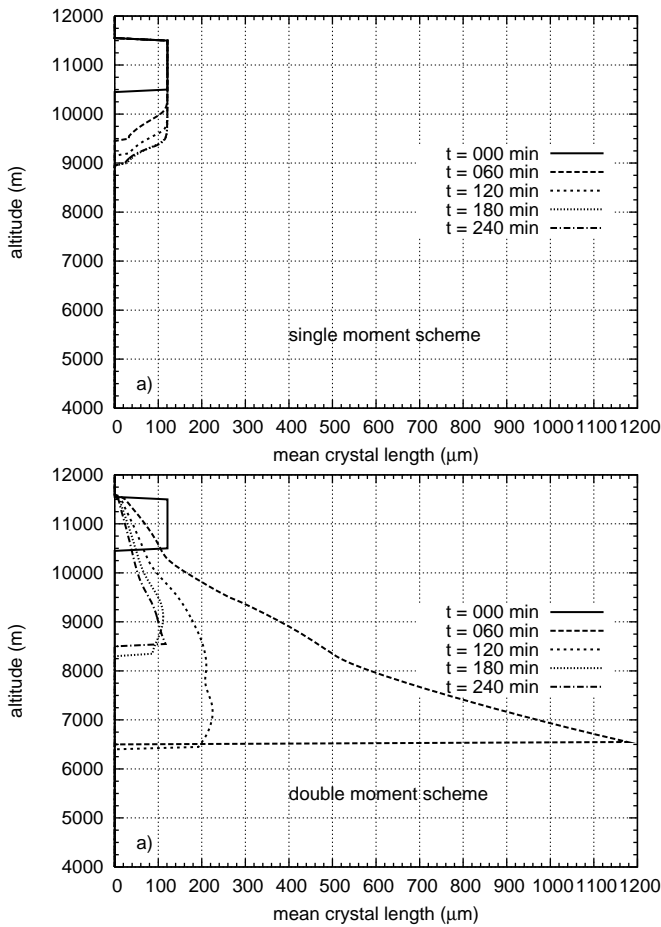


Figure 1: Mean ice crystal lengths vs. altitude in the reference simulations for each hour; top: single moment scheme, bottom: double moment scheme

top and increasingly larger crystals towards cloud bottom and, in particular, fallstreaks evolve beneath the cloud with large crystals, which is not at all the case in the simulation with the single-moment scheme. The crystals that remain within the initial cloud layer are 30 to 120 μm in length, while the larger ones fall out. This result agrees well with our expectation from the physical fact that large crystals fall faster than smaller ones. After one hour the crystals in the fall streak get smaller, a consequence of their evaporation in the subsaturated air. An additional effect can be observed: Due to evaporation, the larger crystals at the bottom of the cloud shrink, hence they fall

velocity becomes smaller. Above them, larger crystals fall down, hence we can observe how some crystals below are larger than the ones on the bottom. This feature, which also can be observed in nature, can be easily seen in Fig. 1.

We have also carried out several sensitivity studies on the impact of different width of the ice crystal mass distribution, cloud layers at different altitudes and with different initial ice water content. In principle, we could find the described characteristics of the different sedimentation schemes for each of these cases (see detailed discussion in Gierens et al., submitted to Quart. Jour. Roy. Met. Soc.).

4. Impact of different sedimentations schemes on radiation

The optical thicknesses for the two reference clouds is given in fig 2. For determining the optical properties (e.g.

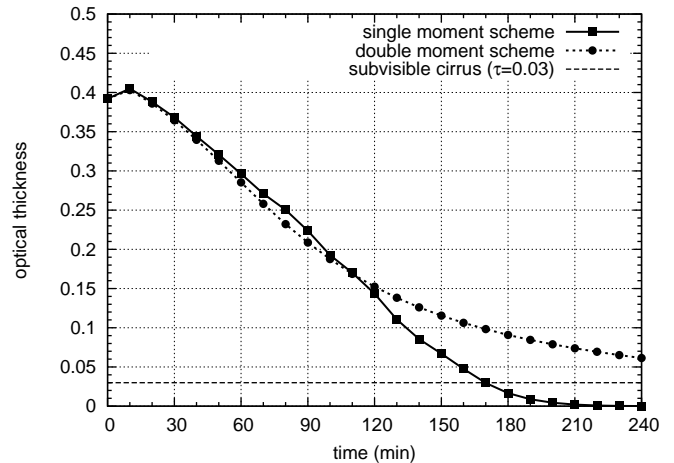


Figure 2: Cloud optical thickness vs. time in the pair of reference simulations

optical thickness) of the simulated clouds we use the formulation of the effective radius as described in Ebert and Curry (1992), assuming columnar crystal shape. The necessary aspect ratios of the columns are computed according to Heymsfield and Iaquinta (2000). The radiation code used in this study is the radiative transfer code

of the CCCma single column model (SCM; Lohmann et al. 1999).

Here we use the ice crystal effective radius and the ice water content from EuLag in 67 levels (interpolated to 200 meter increments from the surface to 12 km and with the standard CCCma levels above) as input parameters for the radiation code. The SCM uses the temperature, specific humidity, ice water content and effective radius as input and assumes that the cloud fully occupies a layer, i.e. the fractional cloud cover for this model is 1 (which is no problem since EuLag is run as a single-column model). For atmospheric trace gases and albedo, reference values from the ARM site in Oklahoma are used. We use a solar zenith angle of 60° . Both clouds get optically thinner during the 4 hr simulation time. While the variation of the optical thicknesses with time is similar in both cases until $t_0 \approx 120 \text{ min}$ into the simulations, there arise larger differences after that time, when the cloud treated with the double-moment sedimentation scheme continues to get optically thinner at a much smaller rate than its counterpart cloud. The cloud that was treated with the double-moment sedimentation scheme remains visible during the whole simulation time, i.e. for at least one hour more than the other cloud.

Although the optical thickness behaves similar for both sedimentation schemes initially, the vertical structure for the optical properties in the two simulated cloud layers is different: As we have seen earlier, there are strong differences in ice water content and crystal number densities, resulting in different vertical profiles of effective radius, local extinction coefficients and other optical parameters. Hence, in spite of similar overall optical thickness, the two clouds differ greatly when considering the heating rate profiles. In order to show this more clearly we consider only the heating rates induced by the clouds by taking the difference full heating rates (with clouds) minus clear sky heating rates. Figure 3 shows the net heating rates for both reference simulations and their corresponding differences. The net rates differ between the two simulations by up to 5 K/d in some cloud layers. Such largely different local heating rates would, in turn, lead to large variations in the dynamic and microphysical response to the radiative effects, but such important feedbacks are currently beyond the capability of our cloud model, and are therefore not further discussed here.

We have also investigated the optical properties for the

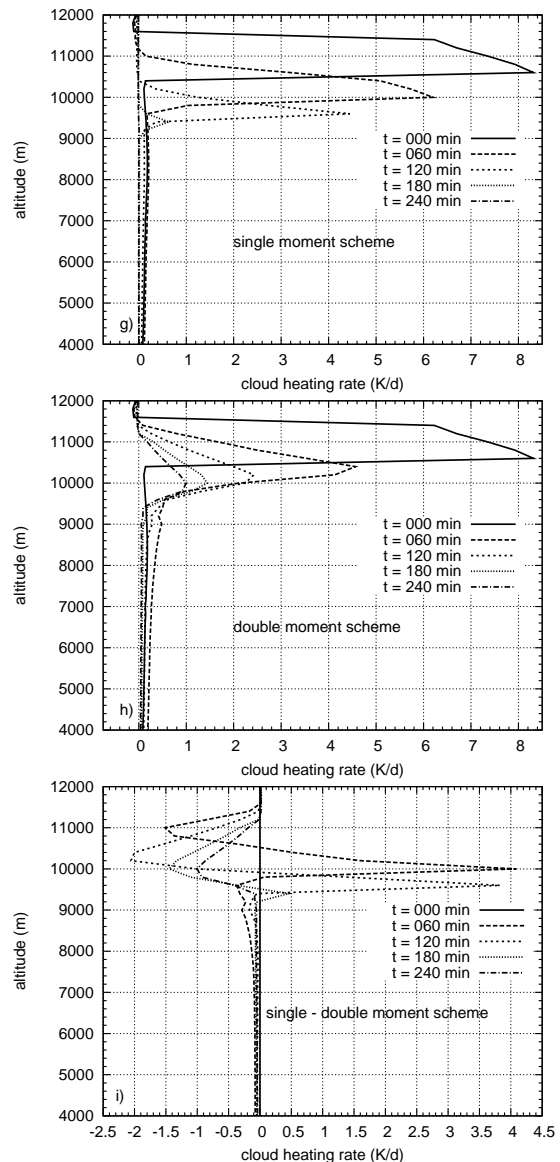


Figure 3: Cloud radiative heating and cooling rate vs. altitude in the two reference simulations at every hour; top: single moment scheme, middle: double moment scheme, bottom: difference single - double.

sensitivity studies mentioned above, but the same statements hold for the optical properties in the different simulations: The heating rates and the optical thickness show

qualitatively the same behaviour.

5. Summary and outlook

In this study we have derived terminal velocities for mass and number concentrations from a flux density concept. We have then tested a double-moment bulk ice microphysics scheme against a single-moment scheme with respect to its microphysical and optical effects. The test consisted in a comparison of a pair of simulations of an initially 1 km thick cirrus cloud.

The double-moment sedimentation scheme lets larger crystals accumulate at cloud bottom while small crystals remain at the cloud top, which is in agreement with many observations (e.g., Heymsfield and Iaquinta, 2002). In contrast, the simple method leads to a cloud with rather uniform crystal size distribution throughout the depth of the cloud, which is contrary to our physical understanding.

Also the life time of the double-moment cloud was larger than that of the single-moment cloud. This fact was also evident in the optical properties, where the single-moment scheme lead to an invisible cloud after about 3 hr whereas the cloud modelled with the double-moment scheme remained visible throughout the 4 hr simulation period. Although the optical thicknesses of the clouds were similar for the first two hours of simulation, the clouds had largely differing vertical structures (distributions of ice mass, hence extinction etc.). This lead to large differences in shortwave, longwave, and net cloud heating rates (within the cloud layer up to 5 K/d), which, when fed back into the dynamics would certainly increase the differences between the two clouds simulations.

The simple process studies have shown great differences in the resulting clouds, their microphysical properties, their vertical structure, lifetime, and optical properties. In particular the latter points show that these effects may be of great importance for climate models and the treatment of sedimentation therefore deserves great care in large-scale models. In agreement with Wacker and Seifert (2001) we have found that double-moment sedimentation is superior to single-moment sedimentation. However, not only the microphysical properties but also the radiative properties of cirrus clouds are strongly

affected by different sedimentation schemes. Our recommendation is therefore to use different terminal velocities for mass and number density as soon as a model makes the step forward to double-moment bulk cloud physics.

Acknowledgement We thank Piotr K. Smolarkiewicz for sharing his model and many fruitful discussions. The numerical simulations were performed on the high performance computer facilities at the European Centre for Medium-Range Forecasts during the special project "Ice supersaturation and cirrus clouds".

References

- Clark, T. L. and Farley, R. D., 1984: Severe downslope windstorm calculations in two and three spatial dimensions using anelastic interactive grid nesting: A possible mechanism for gustiness. *J. Atmos. Sci.*, **41**, 329–350.
- DelGenio, A. D., 2002: 'GCM simulations of cirrus for climate studies'. pp. 310–326 in *Cirrus*. Eds. D. K. Lynch, K. Sassen, D. O'C. Starr, and G. Stephens, Oxford University Press, Oxford, UK.
- Ebert, E. E. and Curry, J. A., 1992: A parametrization of ice cloud optical properties for climate models. *J. Geophys. Res.*, **97**, 3831–3836.
- Ghan, S. J., Leung, L. R., Easter, R. C. and Abdul-Razzak, H., 1997: Prediction of cloud droplet number in a general circulation model. *J. Geophys. Res.*, **102**, 21777–21794.
- Gierens, K. M., 1996: Numerical simulations of persistent contrails. *J. Atmos. Sci.*, **53**, 3333–3348.
- Heymsfield, A. J., 1972: Ice crystal terminal velocities. *J. Atmos. Sci.*, **29**, 1348–1357.
- Heymsfield, A. J. and Iaquinta, J., 2000: Cirrus crystal terminal velocities. *J. Atmos. Sci.*, **57**, 916–938.
- Jakob, C., 2002: 'Ice clouds in numerical weather prediction models'. Pp. 327–345 in *Cirrus*. Eds. D. K. Lynch, K. Sassen, D. O'C. Starr, and G. Stephens, Oxford University Press, Oxford, UK.

- Kajikawa, M. and Heymsfield, A. J., 1989: Aggregation of ice crystals in cirrus. *J. Atmos. Sci.*, **46**, 3108–3121.
- Khvorostyanov, V. I. and Sassen, K., 2002: 'Microphysical processes in cirrus and their impact on radiation'. Pp. 397–432 in *Cirrus*. Eds. D. K. Lynch, K. Sassen, D. O'C. Starr, and G. Stephens, Oxford University Press, Oxford, UK.
- Koenig, L. R., 1971: Numerical modeling of ice deposition. *J. Atmos. Sci.*, **28**, 226–237.
- Lohmann, U., McFarlane, N., Levkov, L., Abdella, K. and Albers, F., 1999: Comparing different cloud schemes of a single column model by using mesoscale forcing and nudging technique. *J. Climate*, **12**, 438–461.
- Lohmann, U., 2002: Possible aerosol effects on ice clouds via contact nucleation, *J. Atmos. Sci.*, **59**, 647–656.
- Lohmann, U. and Kärcher, B., 2002: First interactive simulations of cirrus clouds formed by homogeneous freezing in the ECHAM GCM. *J. Geophys. Res.*, **107**, 4105, doi:10.1029/2001JD000767.
- Smolarkiewicz, P. and Margolin, L., 1997: On forward-in-time differencing for fluids: an Eulerian/Semi-Lagrangian non-hydrostatic model for stratified flows. *Atmosphere-Oceans*, **35**, 127–152.
- Srivastava, R. C., 1978: Parameterization of raindrop size distributions. *J. Atmos. Sci.*, **35**, 108–117.
- Starr, D. O'C. and Cox, S. K., 1985: Cirrus clouds. Part I: Cirrus cloud model. *J. Atmos. Sci.*, **42**, 2663–2681.
- Wacker, U. and Seifert, A., 2001: Evolution of rain water profiles from pure sedimentation: Spectral vs. parameterized description. *Atmos. Res.*, **58**, 19–39.